A New Matrix Decomposition Framework for Specular Reflection Removal from Endoscopic Images

Jithin Joseph[1,*], Sudhish N. George[1] and Kiran Raja[2]

[1]*National Institute of Technology Calicut, Kerala, India*

[2]*Norwegian University of Science and Technology, Norway*

Abstract

Endoscopic images typically suffer from various image degradation such as specular reflection and motion blur due to camera motion. In this paper, we propose a new matrix decomposition method to eliminate the presence of specular reflections (highlights) from endoscopic images. The proposal combines the characteristics of specular reflections and the features of dimensionality reduction through singular value thresholding (SVT) to obtain a highlight free image. Addition of specular reflections with an image alters the singular values of the image matrix. The algorithm iteratively eliminates the changes that occurred to various singular values until all the highlight pixels are eliminated. In order to avoid any loss of significant information, slicing operation is performed on the residue image matrix remained after the initial process. The useful information is extracted from this residue matrix and reinserted with the semi-low-rank component obtained in SVT operation. The experiments and tests reveal that this new matrix decomposition method eliminates the specular reflections from the endoscopic images.

Keywords

Specular Reflections, Singular Value Thresholding, Intensity and Saturation Slicing

1. Introduction

Over the years, endoscopy has evolved as one of the necessary tools used in the medical diagnostic domain. It spreads its branches into colonoscopy, bronchoscopy, esophagoscopy, etc.[1] which are used to view various parts of the internal human body. However, the small intestine is the essential region in the gastrointestinal (GI) tract that stands inaccessible by the conventional tube-like endoscope. As the small intestine is a very long tubular structure arranged in the lower abdominal cavity with numerous bends and folds, it is challenging to use a tube-like structure to view the internals of the small intestine.

The images obtained from the endoscopy may not be ideal as they contain numerous artefacts like the presence of specular reflections (also called highlights), blurred out regions, over-exposed and under-exposed pixels, presence of bubbles and debris, chromatic aberrations, etc. [2]. So it is necessary to remove these artefacts before further analysis.

Highlight removal has been a widely researched topic over the last few years, with several different approaches proposed by many researchers [2][3][4][5][6][7]. These include both supervised and unsupervised approaches achieved in single stage or multiple stages of operation(s).

In the section below, we present a set of related works in this regard.

1.0.1. Highlight Detection:

Many of the early algorithms considered the highlight removal as a two-stage process. The first stage tries to identify the highlight pixels, and in the next stage, the identified pixels are removed and replaced with new information derived from the image itself. In [8], the chromatic difference between the normal pixel and highlight pixel is used to identify the corresponding pixels. Since the reflection from any surface can be considered as two components, viz. diffuse and reflection components [9], the detection of the above components leads to the detection of the highlighted pixel. The diffuse component follows body colour, and the reflection component follows illuminant colour [4]. So by the method of colour channel thresholding or Y-channel thresholding [3], highlight pixels can be identified. In another approach proposed by Kim *et al*. [10], the difference in the polarisation of diffuse and specular reflections is used to identify the highlight pixels. But the database requirement for extracting polarisation characteristics limits this method. In [11], Oh *et al*. identified highlight pixels as characterised by low saturation and high-intensity values, and in [8] this information is used to identify highlight pixels.

1.0.2. Highlight Removal:

Highlight removal can be accomplished either by first performing the highlight detection followed by highlight removal or by performing removal without the prior detection.

(i). *Filter based Approaches* : The whole image can be split into reflection and diffusion components. The diffusion component varies very slowly, whereas the reflection component varies rapidly. In [5], Yang *et al* suggested a filter-based approach to eliminate the high frequency, noisy reflection component with the help of an edge-preserving, low pass filter. Unfortunately, the filtering approach works well only when the frequency of the reflection component is very high, which means this method fails whenever there is a large area of highlight region present. Also, the underlying information lost due to highlight pixels are not being recovered.

(ii). *Chromaticity based Approaches* : In this approach [4][9][12], each of the image pixels is assumed to be consisting of two components rather than assigning individual pixels to a single component. The illuminant colour and tissue colour are extracted and are used to obtain a more reliable colour for each pixel. By properly decomposing the original image, the diffused component is the reflection-free component. As this method highly relies on the object material and motion, it is not suitable for dynamic images.

(iii). *Image Inpainting Methods* : Generally, these techniques are used after highlight detection. Once the highlight pixels are identified, these are inpainted with proper values [6]. Then, window-based approaches are used to inpaint the highlight pixels. Finally, in [13], a structural similarity-based inpainting method is proposed.

(iv). *Data Driven Learning Methods* : Supervised learning approaches show higher efficiency in specularity removal [14][15][16]. The unavailability of labelled data puts restrictions on the training of various networks. In [15], Bobrow *et al*. used pairs of coherent and incoherent images for training. The Conditional Generative Adversarial Network (cGAN) considers

removing the specularity as a translation from image to image. Funke *et al.* [16] proposed the use of two GANs for self-training and self-regularization. The SpecGAN proposed in [16], trains the network from weakly labelled training data.

(v). *RPCA based methods* : Robust Principal Component Analysis (RPCA) is a powerful tool to be used with unlabelled data. The highlight regions are considered a sparse component, and the highlight free image is the low-rank component embedded in the endoscopic image [8]. RPCA has been used in many applications where the low rankness can be employed to extract some features of the original data as in [17][18][8]. The setting of hyperparameters for individual scenes makes the RPCA a time-consuming procedure. In [8], Li. *et al.* proposed a multistage, RPCA based algorithm to remove the highlight from endoscopic images. An adaptive iterative method identifies the parameters that best reduce the specularity in [8], Li. *et al.*. This extra step leads to increased time complexity. Also, the sparse components may contain some useful features. But the problem with RPCA method of specular reflection on endoscopic images is the distribution of highlight pixels. If the highlight pixels are smooth and continuous, they no longer can be considered sparse components. Further, in high-resolution images, the highlight regions contain more pixels which calls for a large correlation between highlight pixels. Here also, the algorithm fails.

This paper proposes a matrix decomposition method to remove the specular reflections from endoscopic images to obtain high-quality images. The proposed method overcomes a lot of demerits of conventional highlight removal algorithms. The merits of the proposed algorithm are listed below.

- The proposed approach eliminates the need for a large labelled dataset as it is not training driven.
- The proposed approach does not require pre-detection of highlighted pixels.
- The approach does not demand scene-wise tuning of parameters, unlike other works [19][14][20][21].
- The sparse information vital for endoscopic images is not lost within the proposed approach.

In addition to these merits, the algorithm provides a fast rate of convergence by applying the characteristics of highlight pixel in the update equations.

The remainder of the paper is structured as follows. Section 2 discusses the mathematical preliminaries required to better understand the proposed method. The proposed new matrix decomposition method for specular reflection removal is outlined in Section 3. The experimental results are presented in Section 4. Finally, the conclusions and future scope are drawn in Section 5.

2. Mathematical Preliminaries

In this section, we briefly explain some of the mathematical ingredients which are necessary for the development of the proposed method.

2.1. Singular value decomposition (SVD)

It is an important mathematical tool used to factorize an M×N matrix [22]. It decomposes a matrix into three sub-matrices as shown in Fig. 1. The SVD of an M×N matrix is given as,

$$\mathbf{X}_{M \times N} = [\mathbf{U}]_{M \times r}[\Sigma]_{r \times r}[\mathbf{V}]_{r \times N}, \quad r = \min\{M, N\} \tag{1}$$

where, $[\mathbf{U}]_{M \times r}$ is the matrix of orthonormal eigenvectors of $\mathbf{AA}^T$. $[\mathbf{V}]_{r \times N}$ is the matrix of orthonormal eigenvectors of $\mathbf{A}^T \mathbf{A}$. $[\Sigma]_{r \times r}$ is the diagonal matrix of the singular values which are the square roots of the eigenvalues of $\mathbf{A}^T \mathbf{A}$.

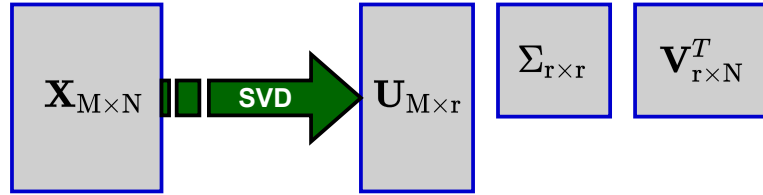**Figure 1:** Singular Value Decomposition

2.2. Soft thresholding operator

Soft thresholding of a matrix is used to discard insignificant elements of the matrix with reference to some threshold. Along with discarding these elements, it also reduces the strengths of other elements also. The operator is defined as [23],

$$\mathcal{S}_\tau(\mathbf{X}) = [\mathcal{S}_\tau(x), \quad \forall x \in \mathbf{X}] \tag{2}$$

$$\mathcal{S}_\tau(x) = sgn(x) \times \max\{x - \tau, 0\}$$

2.3. Singular value thresholding operator

SVT operator works in two stages. In the initial stage, it performs the SVD operation on the image matrix. Then, the soft thresholding is performed on the singular value matrix. The reconstructed matrix using the modified singular values is the result of this operation. Mathematically, we can represent the operation as follows [23]:

$$\mathcal{D}_\mu(\mathbf{X}) = \mathbf{U}\mathcal{S}_{\frac{1}{\mu}}(\Sigma)\mathbf{V}^T \tag{3}$$

where, $\mathbf{X} = \mathbf{U}\Sigma\mathbf{V}^T$ is the singular value decomposition of the matrix $\mathbf{X}$, with Σ being the singular value matrix.

3. Proposed Method

In the proposed method, the specular reflection components embedded in the endoscopic image is removed by applying a new matrix decomposition technique. The original endoscopic image

(**M**) is decomposed into a semi-low-rank component (**L**) and a highlight component (**H**) as follows.

$$\mathbf{M} = \mathbf{L} + \mathbf{H} \tag{4}$$

If we attempt to decompose the matrix into a truly low-rank component and a sparse component as in RPCA [24], many of the highlight pixels will be removed from the original image **M**. But the highlight component of the image cannot be perfectly sparse in nature. It contributes significantly to the low rank component of the image. In addition, there can be some sparse non-highlight information making the component **L** a semi-low-rank component.
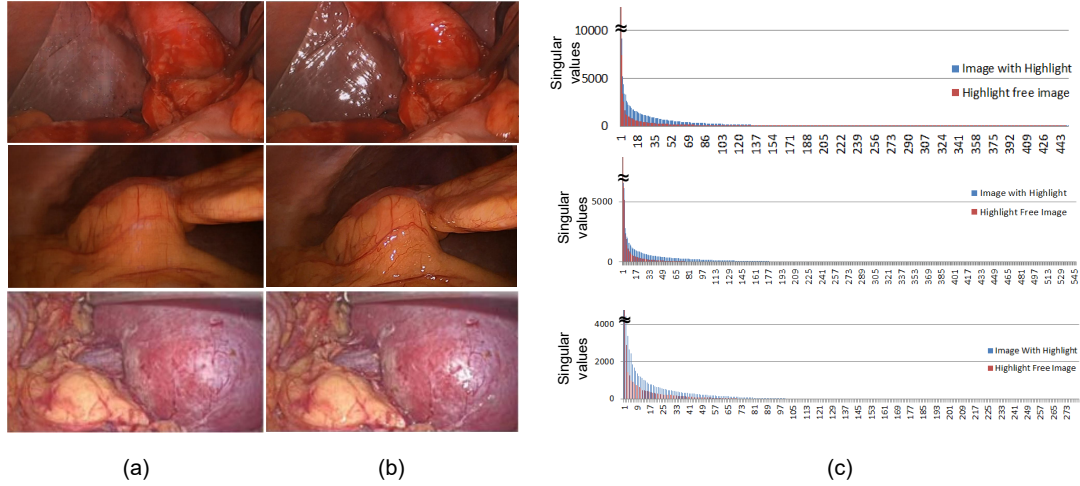

Figure 2: Singular value Distribution. (a) Highlight Free Images, (b) Images with Highlight added and (c) Singular value distribution for the 2 kinds of images.

Fig. 2 shows the change in singular values of a highlight free image by the addition of highlight components. All the observations lead us to conclude that specular components contribute to every singular values. So the removal of specular components is an iterative procedure in which singular values are iteratively reduced until a good highlight free image is obtained. Thus, we take advantage of singular value decomposition and singular value thresholding of the image matrix with the chromatic characteristics of the highlight pixels to obtain the semi-low-rank component.

3.1. Obtaining the semi-low-rank component

The key idea to obtain the semi-low-rank component is to extract details out of the original endoscopic image iteratively until all the specular components are removed completely. Removing all specular components in a single step needs to subtract the exact contribution of the specularity in each of the singular values. Extracting this information from the original image is practically not possible. Further, the contribution differs from image to image. So the solution becomes an iterative procedure that can converge when all the specularities are removed. Thus, the algorithm can be summarized as below:

Algorithm 1: Basic steps followed in the proposed method

1. Perform the singular value decomposition of the original image.
2. Apply the 'soft thresholding operator' on the singular values to reduce the contribution of specularity on them.
3. Reconstruct the image to obtain the semi-low-rank component.
4. Check for convergence. If not converged, repeat from step 1.

The steps 1, 2 and 3 can be performed by the use of 'singular value thresholding operator' defined in Eq. (3). Thus the extraction operation is given by,

$$\mathbf{L} = \mathcal{D}_\mu(\mathbf{M}) \tag{5}$$

The part of $\mathbf{M}$ remaining after the formation of $\mathbf{L}$ is the residue matrix represented as $\mathbf{H}$, which is expected to contain only the highlight component.

$$\mathbf{H} = \mathbf{M} - \mathbf{L} \tag{6}$$

While the algorithm outlined appears to result in highlight component alone, we not that it does not always hold true. This observation can be argued with the reasons listed below:

i. There is useful information in an endoscopic image that may be considered sparse. These components have contributions towards the least significant singular values. Applying soft thresolding technique removes this information and will be accumulated on $\mathbf{H}$.

ii. In order to remove specularity completely, proper selection of the parameter μ is essential. If μ is selected high, $\frac{1}{\mu}$ becomes less and only purely sparse components will be removed and it takes more time. So the value of μ must be very low. But in that case, there is a possibility of relevant information also get removed due to the 'higher step size'.

This implies that in each iteration we remove both highlight pixels and some relevant information using a very small value of μ. The decomposition is given in Fig. 3.
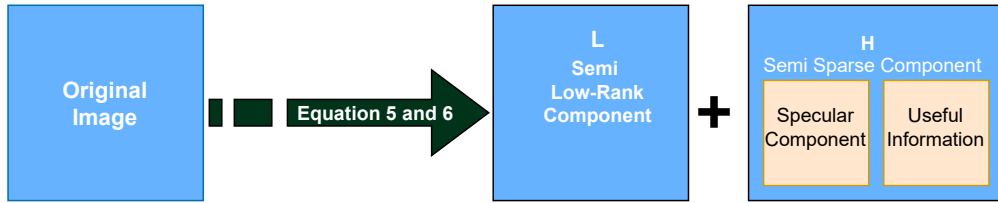

Figure 3: Decomposition procedure

Now the $\mathbf{H}$ component contains both highlight pixels and useful information. We proceed to extract this useful information from $\mathbf{H}$ and reinsert the same into $\mathbf{L}$, so that the highlight component will be available in $\mathbf{H}$ and the remaining in $\mathbf{L}$.

3.2. Separating the specular component from the useful information

The component remaining after the initial step is, $\mathbf{H} = \mathbf{M} - \mathbf{L}$. Our method of extracting the specular components from $\mathbf{H}$ is as follows. All the pixels in the image $\mathbf{H}$ are made zero if they are not following the characteristics of specular reflections. Then the remaining component represents only the specular reflection, i.e., for $\forall\, h \in \mathbf{H}$,

$$
\text{S'}(h) \;=\; \begin{cases} h, & \text{whenever } h \text{ is a highlight pixel} \\ 0, & \text{otherwise} \end{cases} \tag{7}
$$

That is, S'(h) is thresholding operation.

Each pixel h is decided to be a highlight pixel by applying the characteristics of highlight pixels [11]. In HSV color space, a pixel is assigned as a highlight pixel according to the function defined as,

$$
\text{ishighlight}(h = (h_H, h_S, h_V)) = \begin{cases} +1, & \text{if } h_S < T_S \text{ and } h_V > T_V \\ 0, & \text{otherwise} \end{cases} \tag{8}
$$

where, T_S is the threshold for saturation channel and T_V is the threshold for the intensity channel. For the RGB color space, the decision rule is stated for a single channel as,

$$
\text{ishighlight}(h_i = (h_H, h_S, h_V)) = \begin{cases} +1, & \text{if } h_i > T_i \\ 0, & \text{otherwise} \end{cases} \tag{9}
$$

$\forall\, i \in [R, G, B]$.

The threshold for each channel is obtained from the image under processing using the following equation.

$$
T_i \;=\; mean(\text{channel}_i) \;+\; \beta \times std(\text{channel}_i), \quad \forall i \in [\text{ R, G, B }] \tag{10}
$$

where, $mean$ and std are the statistical mean and standard deviation of the channel in image $\mathbf{H}$ respectively. Applying Eq. (9) and (10) in Eq. (7) yields the operation required to extract highlight pixels from the image $\mathbf{H}$. Clearly the operation obtained is simply the intensity level slicing operation. The thresholds are obtained from Eq. (10).

Now the operation performed for obtaining only the highlight pixels from $\mathbf{M} - \mathbf{L}$ is,

$$
\mathbf{H} \;=\; \text{Slicing}(\mathbf{M} - \mathbf{L}) \tag{11}
$$

The slicing operation is defined as,

$$
\text{Slicing}(\mathbf{H}) \;=\; [\; \text{S'}(h), \quad \forall\, h \in \mathbf{H} \;] \tag{12}
$$

where,

$$
\text{S'}(h) = \text{ishighlight}(h) \times h
$$

Once the highlight-only image **H** is obtained, the remaining component is given by **M** - **L** - **H**. Let it be **Y**. This is the useful information that must reside in the semi-low-rank component. Now this term is added back to **L**, so that in the next iteration, new value of **L** is obtained by the singular value thresholding operation on (**L** + **Y**) = (**M** - **H**). The update equations for the semi-low-rank component and the highlight component can be summarised as,

$$\begin{aligned} \mathbf{L}^{k+1} &= \mathcal{D}_\mu(\mathbf{M} - \mathbf{H}_k) \\ \mathbf{H}^{k+1} &= \text{Slicing}(\mathbf{M} - \mathbf{L}_{k+1}) \end{aligned}$$

(13)

The above mentioned iterative procedure is repeated until (**M** - **L** - **H**) becomes insignificantly small. That is $\|\mathbf{M} - \mathbf{L} - \mathbf{H}\|_F^2 \ <= \ \zeta$, where $\|.\|_F^2$ is the Frobenius norm. Resulting **L** contains all the features other than specular reflections and **H** contains all the highlight regions. The entire procedure is outlined in Fig. 4 and steps are enumerated in Algorithm 2.

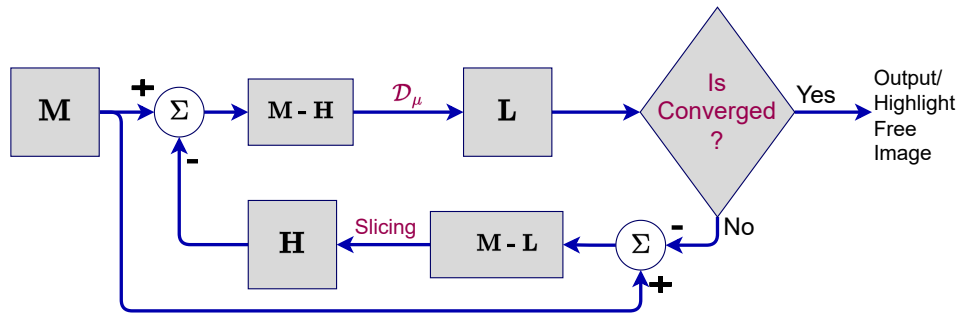**Figure 4:** Proposed method

---

Algorithm 2: Removing Highlight components from WCE images
---
1. **Input: M** $\in \mathcal{R}^{M \times N \times 3}$
2. **Output: L** $\in \mathcal{R}^{M \times N \times 3}$
3. **Initialize: L, H, Y = 0,** μ = 0.001
4. Read Image to **M**.
5. Calculate T_R, T_G, T_B using Eq. (10).
6. Update **L, H** and **Y** according to Eq. (13).
7. Check for convergence. The condition is $\|\mathbf{M} - \mathbf{L} - \mathbf{H}\|_F^2 <= \zeta$. If the condition is satisfied, Algorithm stops and **L** gives the highlight free image. Else repeat from Step 6.

---

4. Experimental Results and Discussions

To evaluate the results obtained from the proposed algorithm, we have performed experiments on two different publicly available datasets - the Kvasir-colonoscopy[1] dataset and the CVC-

---

[1]https://datasets.simula.no/kvasir/

ClinicSpec[2] dataset [3].

The results obtained are validated objectively using the percentage of remaining highlight. We design two experiments to validate the proposed method. In the first experiment, images from two datasets are processed using the proposed method and the percentage of highlight remaining in each image after processing is calculated as given by Eq. 14:

$$\text{Percentage of highlight} = \frac{\text{No. of pixels satisfying the conditions for highlight}}{\text{Total No. of pixels in the original Imge}} \tag{14}$$

A pixel satisfying the conditions for highlight is decided by Eq. (9). Low value of percentage indicates a high efficiency for the algorithm.

From the Kvasir-colonoscopy dataset, 500 images are selected for testing our algorithm, the resolution of which ranges from 720×576 to 1920×1072. All of the images contain significant specular reflections. Fig. 5 shows the result of the first experiment, and only two images from each dataset are shown for the sake of illustration. The first two rows are the images from the Kvasir-colonoscopy dataset, and the remaining two rows are the images from the CNC-ClinicSpec dataset. Despite the images from different datasets, the output of the proposed approach is observed to be consistent. However, it is observed that the boundaries of the highlight pixels in the original image remain. The boundaries are defined by the shadow regions created by the illumination, and these dark regions are clearly visible in the enlarged view of the original image.

As part of the first experiment, we have calculated the percentage of highlights remaining in different images from two datasets using Eq. (14). The reduction in highlight is shown in Fig. 6 for 5 sample images.

In the second experiment, the proposed method is compared with the state of the art matrix decomposition methods based on singular values. The methods compared are (a) $l^{1/2}$ Regularized RPCA [25], (b) AS-RPCA [26], (c) PCP [24] and (d) FPCP [27]. The comparison is shown in Fig. 7. The corresponding statistical distribution of the percentage of highlights that remained in the final image is presented in Table 1, for the 500 images tested from Kvasir- colonoscopy dataset. As seen from the Table 1, the proposed approach results in a 0.0052% (standard deviation - 9.7714e-06) of highlights remaining as compared to next best performing approach with 0.0276% highlights intact. The obvious advantage of the proposed approach can be seen against PCA based approaches introspected from the Table 1.

Table 1

Mean and Variance distribution of Percentage of Highlight pixels remained in Processed Image for Various Algorithms.

	$l^{1/2}$ RPCA	AS-RPCA	PCP	FPCP	Our Method
Mean	1.739	0.4038	0.8362	0.0276	0.0052
Standard Deviation	0.688	0.2811	0.4699	0.0547	0.00313

---

[2] http://www.cvc.uab.es/CVC-Colon/index.php/cvc-clinicspec/
[3] The experiments are conducted on a computer with Intel(R) Xeon(R) CPUE5-1620 V_2 with 3.7GHz and 8GB RAM and using Python 3.9.
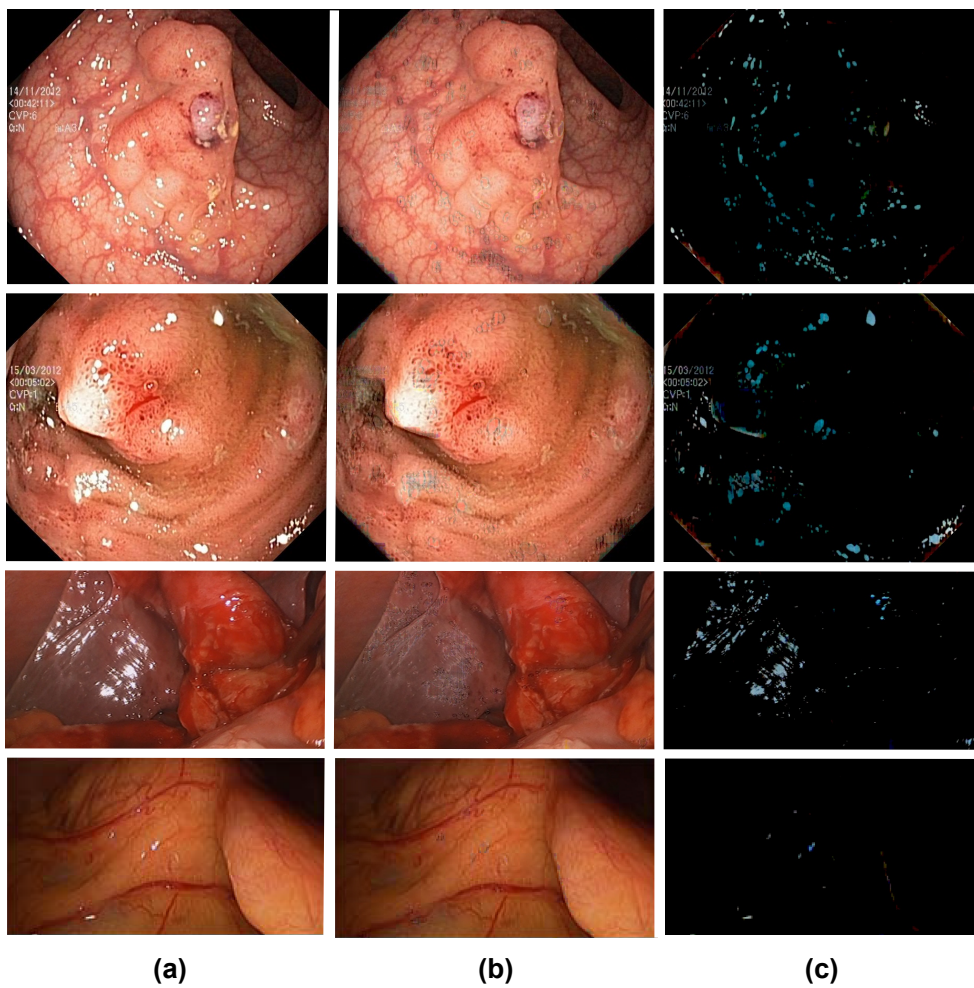
Figure 5: The results of the matrix decomposition proposed (a). Original Image (**M**), (b). Semi-Low-Rank component (**L**) and (c). the highlight component (**H**)
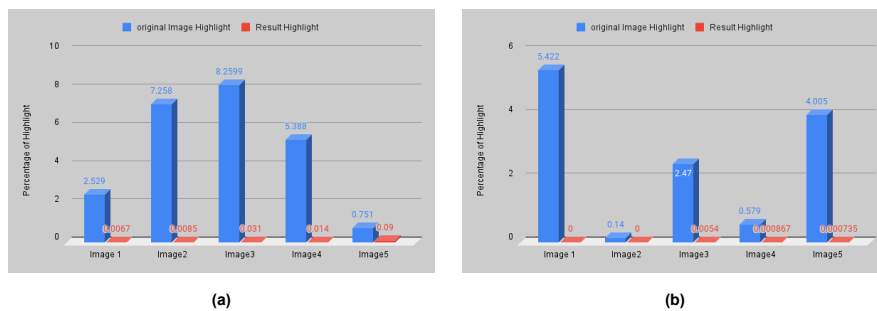

Figure 6: Comparison of percentage of highlight pixels in original input image V output image.(a). Kvasir -Colonoscopy dataset and (b). CVC- ClinicSpec dataset.
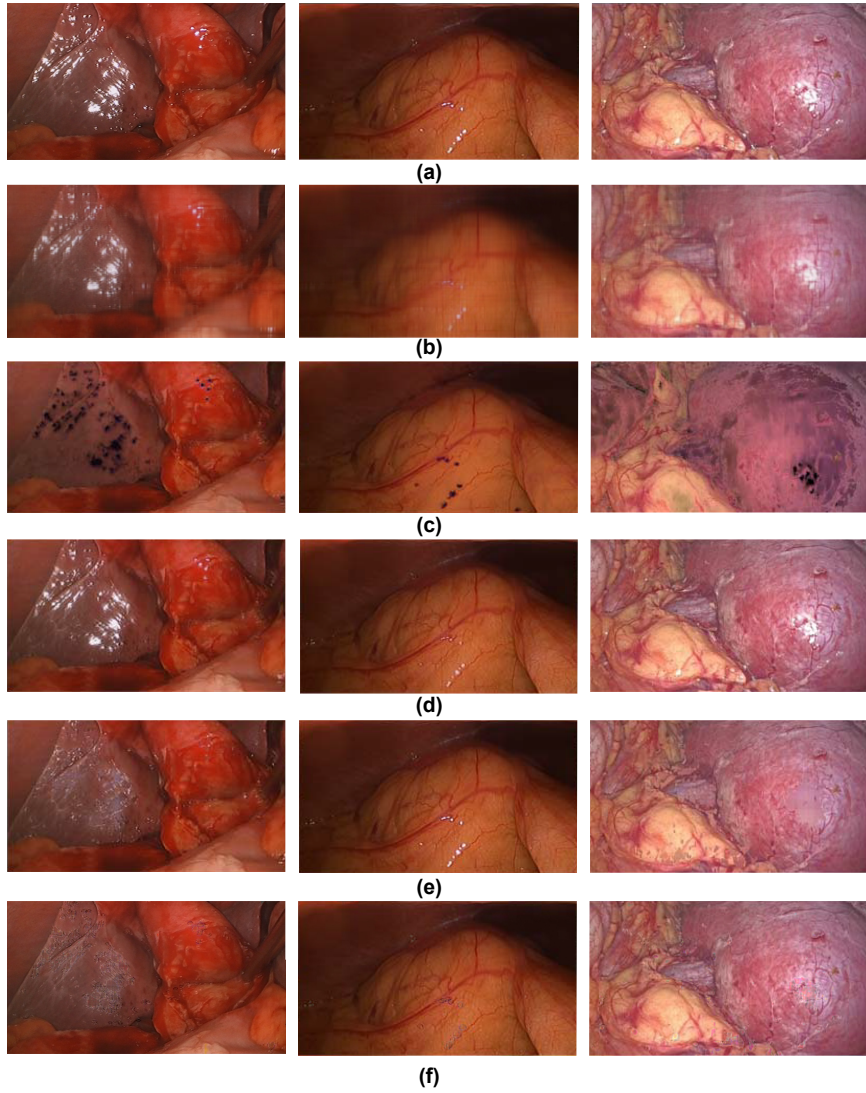
Figure 7: Result of applying various algorithms for highlight removal(a).Original Images, (b) $l^{1/2}$ Regularized RPCA, (c). AS-RPCA, (d). PCP and (e). FPCP and (f) Our Method.

In addition to Table 1, we also conduct the statistical significance analysis using the Box-plots as shown in Figure 8. The obtained results indicate the superiority over the other approaches.

4.1. Time complexity

In addition to quantitative results, we also conduct an analysis for time complexity of the proposed approach as against other state-of-the-art approaches. As seen from the results presented in Table 2, the average time complexity of the proposed approach is significantly lower compared to next best performing approach (i.e.,FPCP). The results indicate that superiority of
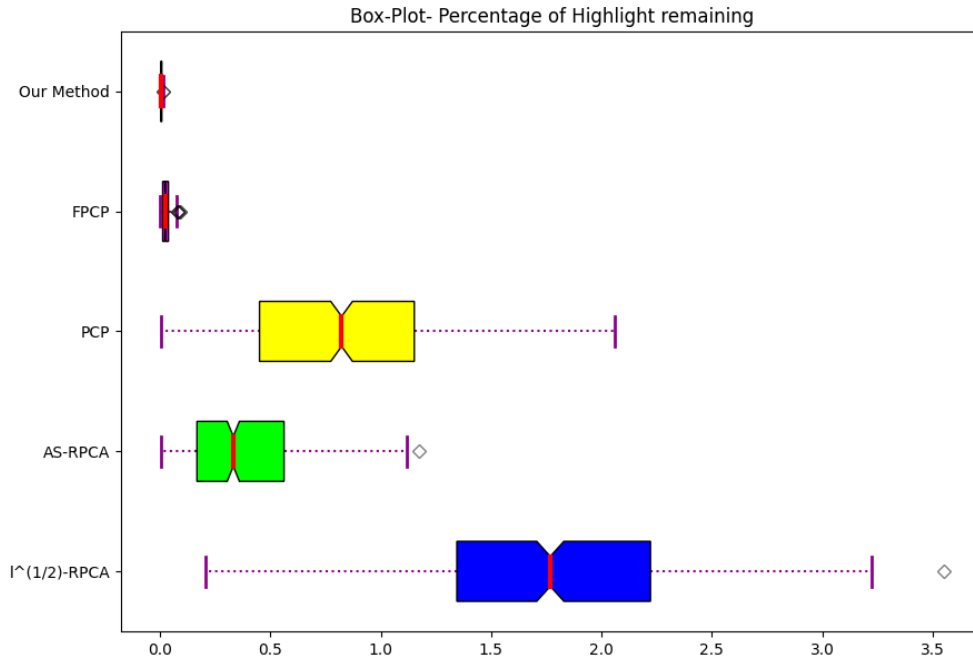
Figure 8: Statistical validation of proposed approach against other state-of-the-art approaches illustrated using Box-plots.

the proposed approach both in terms of highlight removal and time complexity.

Table 2

Execution Time (in seconds) for Various Algorithms. Images from Kvasir-Colonoscopy are used.

	$l^{1/2}$ RPCA	AS-RPCA	PCP	FPCP	Our Method
Mean	14.18	58.63	250.67	8.757	6.1
Standard Deviation	2.5977	10.9006	29.409	1.4713	0.1867

4.2. Limitations of proposed approach

The employed Kvasir-colonoscopy dataset consists of images with padded boundaries due to the nature of imaging. These boundary regions result in pseudo-artefacts and cannot be avoided if the whole image is considered. Better strategies for handling such boundaries are not investigated in this work and will be studied in future works.

References

[1] N. VX, S. R., M. M. E., Appropriate use of endoscopy in the diagnosis and treatment of gastrointestinal diseases: up-to-date indications for primary care providers., International journal of general medicine 3 (2010) 345–57.

[2] S. Ali, F. Zhou, A. Bailey, B. Braden, A deep learning framework for quality assessment and restoration in video endoscopy, Medical Image Analysis 68 (2021) 101900.

[3] W. Lim, Robust specular reflection removal and visibility enhancement of endoscopic images using 3-channel thresholding technique and image inpainting, Technium Romanian Journal of Applied Sciences and Technology 2 (2020) 336–343.

[4] H.-L. Shen, H.-G. Zhang, S.-J. Shao, J. H. Xin, Chromaticity-based separation of reflection components in a single image, Pattern Recognition 41 (2008) 2461–2469.

[5] Q. Yang, S. Wang, N. Ahuja, Real-time specular highlight removal using bilateral filtering, in: ECCV, 2010.

[6] M. Arnold, A. Ghosh, S. Ameling, G. Lacey, Automatic segmentation and inpainting of specular highlights for endoscopic imaging, EURASIP Journal on Image and Video Processing 2010 (2010).

[7] J. Jiao, W. Fan, J. Sun, N. Satoshi, Highlight removal for camera captured documents based on image stitching, in: 2016 IEEE 13th International Conference on Signal Processing (ICSP), 2016, pp. 849–853.

[8] R. Li, J. Pan, Y. Si, B. Yan, Y. Hu, H. Qin, Specular reflections removal for endoscopic image sequences with adaptive-rpca decomposition, IEEE Transactions on Medical Imaging 39 (2020) 328–340.

[9] R. Tan, K. Nishino, K. Ikeuchi, Separating reflection components based on chromaticity and noise analysis, IEEE Transactions on Pattern Analysis and Machine Intelligence 26 (2004) 1373–1379.

[10] D. Kim, S. Lin, K.-S. Hong, H.-Y. Shum, Variational specular separation using color and polarization., 2002, pp. 176–179.

[11] J. Oh, S. Hwang, J. Lee, W. Tavanapong, J. Wong, P. C. de Groen, Informative frame classification for endoscopy video, Medical Image Analysis 11 (2007) 110–127.

[12] T. Tan, K. Nishino, K. Ikeuchi, Illumination chromaticity estimation using inverse-intensity chromaticity space, volume 1, 2003, pp. I–673.

[13] Y. Gao, J. Yang, S. Ma, D. Ai, T. Lin, S. Tang, Y. Wang, Dynamic searching and classification for highlight removal on endoscopic image, Procedia Computer Science 107 (2017) 762–767. Advances in Information and Communication Technology: Proceedings of 7th International Congress of Information and Communication Technology (ICICT2017).

[14] Y. Chang, C. Jung, Single image reflection removal using convolutional neural networks, IEEE Transactions on Image Processing 28 (2019) 1954–1966.

[15] T. L. Bobrow, F. Mahmood, M. Inserni, N. J. Durr, Deeplsr: a deep learning approach for laser speckle reduction, Biomedical Optics Express 10 (2019) 2869.

[16] I. Funke, S. Bodenstedt, C. Riediger, J. Weitz, S. Speidel, Generative adversarial networks for specular highlight removal in endoscopic images, 2018, p. 3.

[17] B. Shijila, A. J. Tom, S. N. George, Moving object detection by low rank approximation and l1-tv regularization on rpca framework, Journal of Visual Communication and Image

Representation 56 (2018) 188–200.

[18] M. S. Subodh Raj, S. N. George, $l^{1/2}$ regularized rpca technique for 3d human action recovery, in: 2020 IEEE 17th India Council International Conference (INDICON), 2020, pp. 1–5.

[19] F. d. S. Queiroz, I. R. Tsang, Automatic segmentation of specular reflections for endoscopic images based on sparse and low-rank decomposition, in: 2014 27th SIBGRAPI Conference on Graphics, Patterns and Images, 2014, pp. 282–289.

[20] G. Fu, Q. Zhang, C. Song, Q. Lin, C. Xiao, Specular highlight removal for real-world images, Computer Graphics Forum 38 (????) 253–263.

[21] J. Guo, Z. Zhou, L. Wang, Single image highlight removal with a sparse and low-rank reflection model, in: Computer Vision – ECCV 2018, 2018, pp. 282–298.

[22] V. Klema, A. Laub, The singular value decomposition: Its computation and some applications, IEEE Transactions on Automatic Control 25 (1980) 164–176.

[23] J.-F. Cai, E. J. Candès, Z. Shen, A singular value thresholding algorithm for matrix completion, SIAM Journal on Optimization 20 (2010) 1956–1982.

[24] E. J. Candès, X. Li, Y. Ma, J. Wright, Robust principal component analysis?, J. ACM 58 (2011).

[25] S. Raj M S, S. George, l 1/2 regularized rpca technique for 3d human action recovery, 2020, pp. 1–5.

[26] G. Liu, S. Yan, Active subspace: Toward scalable low-rank learning, Neural computation 24 (2012).

[27] P. Rodríguez, B. Wohlberg, Fast principal component pursuit via alternating minimization, in: 2013 IEEE International Conference on Image Processing, 2013, pp. 69–73.